International Journal of Mass Spectrometry 309 (2012) 161–167

Contents lists available at SciVerse ScienceDirect

International Journal of Mass Spectrometry

journal homepage: www.elsevier.com/locate/ijms

Analyzing a mixture of disaccharides by IMS-VUVPD-MS

Sunyoung Lee, Stephen J. Valentine, James P. Reilly, David E. Clemmer*

Department of Chemistry, Indiana University, Bloomington, IN 47405, United States

ARTICLE INFO

Article history:
Received 17 May 2011
Received in revised form 11 August 2011
Accepted 15 September 2011
Available online 23 September 2011

Keywords:
UV photodissociation
Collision-induced dissociation
Ion mobility spectrometry
Disaccharide

ABSTRACT

Comparative analyses utilizing collision-induced dissociation (CID) and vacuum ultraviolet photodissociation (VUVPD) for seven isobaric disaccharides have been performed in order to differentiate the linkage type and anomeric configuration of the isomers. Although an individual CID spectrum of a disaccharide ion provides information related to its structure, CID does not sufficiently differentiate mixture components due to the identical mass-to-charge values of most of the intense fragments. In contrast to the ambiguity of the CID analyses for the disaccharide mixture, VUVPD (157 nm) generates unique fragments for each disaccharide ion that are useful for distinguishing individual components from the mixture. When combined with a gas-phase ion mobility separation of the ions, the identification of each component from the mixture can be obtained.

1. Introduction

Carbohydrates play numerous roles in biological systems, from a means of providing energy, to establishment of vital structural elements that allow cellular recognition [1–8]. Unlike linear polymeric chains of amino and nucleic acids, carbohydrate structures can exhibit significant complexity, arising from different monosaccharide residues, multiple linkage positions and anomericities, as well as other factors (e.g., position within a protein fold). Despite tremendous effort, much remains to be understood about these interesting molecules. For example, it is important to determine linkage types and anomeric configurations between the individual residues simply to understand the covalent structures of these molecules.

In this paper, we take a reductionist approach to understanding carbohydrate structure, focusing on characterizing the structures of some of their simplest forms, a series of related disaccharides (that are formally isomers). At first glance, such a simple system would seem trivial for modern techniques; however, its complexity presents significant challenges that make improvements in technologies desirable, and hence a focus of this work. Disaccharides themselves are also important; they are often the products of enzymatic activity (e.g., heparinase and pancreatic amylase activity results in formation of disaccharides) [9,10] and thus, the development of rapid and sensitive techniques that are capable of detailed structural characterization is important for practical applications.

There is a substantial history associated with the use of mass spectrometry (MS) [11–26] for determining the structures of carbohydrates. Collision-induced dissociation (CID) has been extensively applied to differentiate the carbohydrate isomers where the generation of characteristic CID fragmentation related to linkage type and anomeric configuration is useful for elucidating carbohydrate structure [11–15]. More recently, vacuum ultraviolet photodissociation (VUVPD) has also been utilized for detailed structural assignments [23–25]. High-energy dissociation upon UV laser irradiation can lead to the generation of additional cross-ring fragment ions that are instructive for assigning specific branching and glycosidic linkages. Electron capture (and transfer) dissociation methods can also produce cross ring glycan fragments [19,20], and are especially intriguing for structural characterization by MS because these dissociative techniques tend to cleave the peptide backbone (on glycopeptides and glycoprotein complexes) which is useful for locating glycosylation sites along polypeptides [26]. It is interesting that little structural information about the glycan is obtained from these experiments when the glycopeptide form is the precursor ion.

Tandem mass spectrometry (MS^n) analyses of individual carbohydrate ions provide a powerful means of determining many of the details of structures; however, such state-of-the-art methods [13–16] are still challenged when isomers having identical mass-to-charge (m/z) values exist in a mixture. To achieve complete analysis of an isobaric mixture, often a m/z independent separation step is required prior to MS or MS^n experiments. Capillary electrophoresis can be employed as a separation tool, but this often introduces a need to chemically modify molecules such that UV or fluorescence detection schemes can be employed, and the solution conditions that are used in these studies are often incompatible

* Corresponding author.
E-mail address: clemmer@indiana.edu (D.E. Clemmer).

1387-3806/$ – see front matter © 2011 Elsevier B.V. All rights reserved.
doi:10.1016/j.ijms.2011.09.013

with electrospray ionization (ESI) [27,28]. The approach that we examine in this paper uses ion mobility spectrometry (IMS) coupled with MS. We aim to incorporate the powerful MS^n strategies, and hope to improve upon such methods by using the IMS as a means of simplifying the mixture prior to MS analysis. IMS can separate isomeric carbohydrates due to differences in their mobilities in the gas-phase and thus is easily coupled to MS devices [22,29,30]. Here, we also explore VUVPD to generate fragments because it appears to offer advantages for these types of molecules compared with CID.

2. Experimental

2.1. Sample preparation and ionization

All disaccharides used in this study have been obtained from Sigma–Aldrich (St. Louis, MO) and are used without further purification. The seven disaccharides are as follows: gentiobiose (β1–6), melibiose (α1–6), palatinose (α1–6), leucrose (α1–5), cellobiose (β1–4), sucrose (α1–2), and trehalose (α1–1). Singly sodiated ($[M+Na]^+$) disaccharide ions are produced by electrospraying a solution containing 100 μM of the disaccharide in a 50:50 (vol.%) water:acetonitrile and 2 mM NaCl solution. The sample mixture of seven disaccharides is prepared in the same solution to provide a final concentration of 100 μM for each molecule. The samples are infused through a pulled capillary (75 μm i.d., 360 μm o.d.) tip at a flow rate of 300 nL min^{-1} using a syringe pump (KD Scientific, Holliston, MA). The capillary tip is maintained at a DC bias of ~2.0 kV above the voltage of the entrance plate to the desolvation region.

2.2. Ion mobility/mass spectrometry measurements

General aspects of IMS instrumentation, techniques, and theory have been reviewed previously [20,29–38]. For these studies, a home-built ion mobility spectrometer is coupled to a LTQ Velos instrument (Thermo Electron, San Jose, CA). Detailed descriptions of the novel instrument used for the current studies are provided elsewhere [39,40]. Only a brief overview of the experimental methods is presented here. Positively charged ions from the ESI source are focused through an hour glass ion funnel (F1) [41]. The ions are accumulated in the back of F1 and periodically (at a frequency of 55 Hz) extracted into a drift region via an introduction gate. The drift tube is ~1 m long with a uniform electric field of $\sim 2.3 \times 10^3$ V m^{-1} and contains ~3 Torr of an inert buffer gas mixture (N_2 and He). As a narrow packet of ions from the introduction gate travels through the buffer gas, individual ions separate according to differences in their mobilities. After mobility separation, ions are transferred through a second ion funnel (F2) that is used to focus the diffuse ion cloud. To select ions with specific mobilities, a voltage pulse (80 μs width) is applied to a selection gate and the pulse is delayed from the initial ion pulse by a determined amount of time. To obtain the IMS distribution, the ion signal is recorded as the delay time is scanned across the total drift time range (from ~11 to ~18 ms) using time increments of ~80 μs.

It is noteworthy to consider factors affecting the mobility separation of the mixture components. It is possible that potential differences in ion neutral interaction associated with the buffer gas mixture play a role in the mobility separation that is achieved. As noted above, the buffer gas mixture permits the use of significantly higher fields than in drift tubes that utilize ~3 Torr of pure He. For these studies, it is likely that the usage of a higher drift field ($\sim 2.3 \times 10^3$ V m^{-1}) has a greater impact on the relatively high-resolution (compared to longer drift tubes) mobility separation. Mobility distributions obtained for protein, peptide, oligosaccharide, and glycan ions using this 1 m drift tube are similar to those obtained with a 2 m drift tube filled with pure He.

Mobility-selected ions exiting the drift tube enter the LTQ ion trap mass spectrometer. A mass spectrum can also be obtained without mobility separation by turning off the ion gates. Ions are isolated inside the linear trap with a ±1 Th isolation window prior to ion activation. Mobility and/or mass-selected ions are stored in the trap and they can be dissociated by either 157 nm photoexcitation or collisional activation. Details regarding the modified LTQ providing the capability for photodissociation have been reported [24,25,39,40]. Briefly, a F_2 laser (EX100HF-60, GAM Laser, Orlando, FL) has been connected to the rear of the LTQ with a vacuum line. A single pulse of 157 nm light is introduced into the ion trap at the beginning of a 10 ms activation period with 0% normalized collision energy and an activation q of 0.1. For CID experiments, a resonant RF excitation waveform is applied for 10 ms with 25% normalized collision energy and an activation q of 0.25. Photofragment ions of interest are subjected to MS^3 analysis by CID under the same ion isolation and CID conditions as the MS^2 experiments.

3. Results and discussion

3.1. Comparison of CID and VUVPD for individual disaccharides

The MS^2 spectra generated by CID and VUVPD for seven isobaric disaccharides have been examined to evaluate their diagnostic value for differentiation of the isomers. The Domon–Costello nomenclature is used to assign all product ions [42]. Figs. 1 and 2 show MS^2 spectra of electrosprayed $[M+Na]^+$ disaccharide ions obtained using CID and VUVPD, respectively. Additionally, the product ions obtained from CID and VUVPD are listed in Tables 1 and 2, respectively.

Previous work has shown that VUVPD provides more informative product ions than CID for glycan and oligosaccharide isomers [23–25]. Similarly, for the isobaric disaccharides studied here, the VUVPD spectra of individual disaccharide ions show additional cross-ring cleavage ions that are not observed in the CID spectra. As shown in Figs. 1 and 2, more complicated fragmentation patterns arise upon photoexcitation of the $[M+Na]^+$ disaccharide ions compared with collisional activation. For example, VUVPD of the $[M+Na]^+$ sucrose ions produces additional fragment ions at m/z = 231, 261, and 275 originating from nonreducing cross-ring cleavages. In contrast, the CID spectrum of the $[M+Na]^+$ sucrose ions contains only glycosidic cleavage ions at m/z = 185 and 203 (Fig. 1a and Table 1). Likewise, activation of the $[M+Na]^+$ trehalose ions by VUVPD generates additional cross-ring cleavage ions at m/z = 231 and 276. Another unique fragment that is observed in the VUVPD spectrum is associated with the loss of a side chain ($-CH_2OH$) which appears generally at m/z = 334 (m/z = 333 for palatinose). It is noted that several CID fragments, such as the ions at m/z = 185, 275 (with the exception of sucrose) and 305, are not observed in the VUVPD spectra. However, fragment ions related to such ions (m/z = 185, 275) are observed arising at m/z = 186 and 276. The ion at m/z = 186 involves the homolytic cleavage of the linkage bond without the glycosidic oxygen. The fragment at m/z = 276 is due to the reducing cross-ring cleavage (fragmentation involving H-transfer). Thus, the same assignments are used for these ions and designated by a superscripted 1 indicating the difference of +1 Th.

Another unique feature in the VUVPD spectra is the observation of glycosidic cleavage ions with both the reducing and nonreducing outcomes for the glycosidic oxygen occurring at m/z = 201, 202, and 203 (C_1^{-2}/Y_1^{-2}, C_1^{-1}/Y_1^{-1}, and C_1/Y_1, respectively). These ions with the glycosidic oxygen are present in all VUVPD spectra; however, their relative intensities are not the same for all isomers. In fact, the relative intensities of the glycosidic cleavage ions can be used to differentiate anomeric configurations (discussed below). Overall, VUVPD results in comprehensive reducing and nonreducing

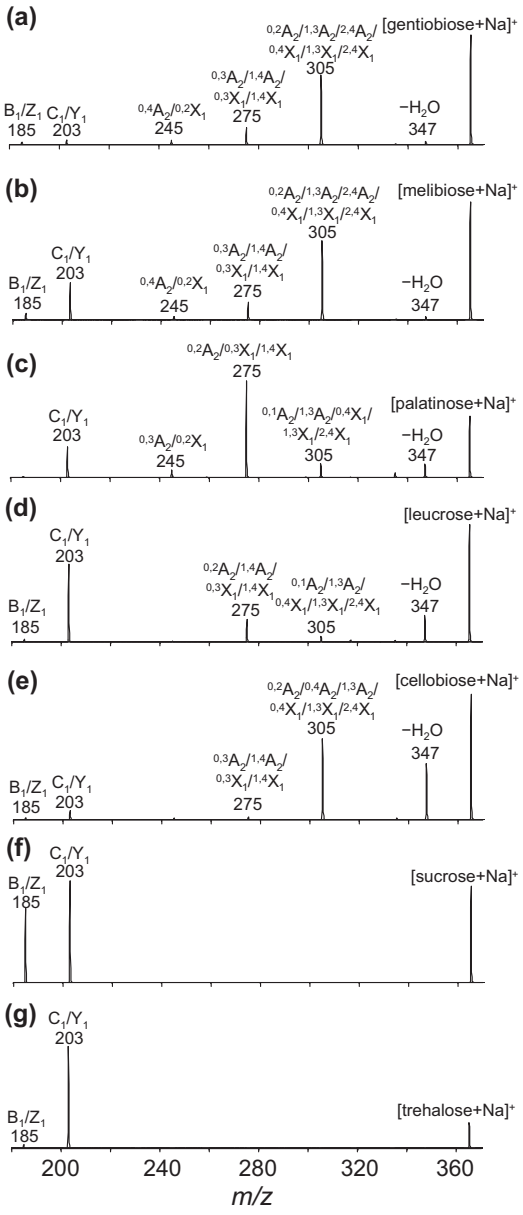

Fig. 1. CID spectra of the $[M+Na]^+$ precursor ions. Spectra shown include: (a) gentiobiose (β1–6); (b) melibiose (α1–6); (c) palatinose (α1–6); (d) leucrose (α1–5); (e) cellobiose (β1–4); (f) sucrose (α1–2); and (g) trehalose (α1–1). Glycosidic cleavage ions (B_1/Z_1 and C_1/Y_1) are observed at m/z = 185 and 203, respectively. Cross-ring cleavage ions are observed at m/z = 245, 275, and 305 corresponding to the loss of $C_2H_4O_2$, $C_3H_6O_3$, and $C_4H_8O_4$ fragments, respectively. Neutral loss of H_2O appears at m/z = 347. All product ions are singly sodiated.

fragments containing glycosidic, cross-ring, and side-chain cleavage ions. Fig. 2 shows possible bond cleavages caused by photofragmentation of the individual disaccharides.

The cross-ring cleavage ions obtained by VUVPD can provide specific structural information for the isobaric disaccharides. All disaccharides except sucrose and trehalose generate a cross-ring cleavage ion at m/z = 259 that indicates the loss of $C_3H_6O_4$. The formation of the fragment ion at m/z = 259 is possible if the precursor ion has OH groups on three ring carbon that are adjacent to each other or to the ring oxygen, or OH and CH_3OH groups on the same ring carbon adjacent to the ring oxygen. As shown in Fig. 2, sucrose has a CH_3OH group next to the ring oxygen instead of an OH group. Thus, the $-C_3H_6O_4$ fragment ions are absent in the VUVPD spectrum of the $[M+Na]^+$ sucrose ions (Fig. 2f). In addition, the product ion at m/z = 229 ($^{3,5}A_2$) is a structurally specific fragment for the $[M+Na]^+$ leucrose ions (Fig. 2d). Based on the structures of the seven disaccharides, only leucrose can undergo loss of $C_4H_8O_5$.

One attractive advantage of the VUVPD approach for characterization of the isobaric disaccharides is the production of distinctive fragments for the individual isomers. For example, the fragment ions at m/z = 184, 261, and 275 are unique for the $[M+Na]^+$ sucrose ions (Fig. 2f and Table 2). The product ion at m/z = 333 ($-CH_3OH$) is only observed for the $[M+Na]^+$ palatinose ions. As mentioned above, the structurally specific fragment at m/z = 229 is a characteristic peak for the $[M+Na]^+$ leucrose ions. The peak at m/z = 319 is unique for both the $[M+Na]^+$ gentiobiose and melibiose ions. These two isomers have identical structures with the exception of the anomeric configuration of the glycosidic bond. Thus, they have very similar VUVPD fragmentation patterns. However, the stereoisomers can be distinguished because α and β anomers have different relative intensity ratios of the peaks at m/z = 202 and 203 (described below). Below we show that these unique fragments are useful for identifying individual components within a mixture of the seven disaccharides.

3.2. Differentiation of linkage isomers by MS^2 analysis of individual disaccharides

Previous studies have shown that CID fragmentation patterns depend on the linkage type of isomeric sugars [11,12]. Similarly, the CID spectrum for each of the seven disaccharides (analyzed individually) exhibits linkage-type dependent fragment ions. Two major dissociation pathways for both the 1–1 and 1–2 linked disaccharides, trehalose and sucrose, respectively, are glycosidic cleavages producing a nonreducing ring without the glycosidic oxygen (B_1/Z_1 at m/z = 185) and the reducing end of a glycosidic cleavage ion (C_1/Y_1 at m/z = 203). The 1–4 (cellobiose), 1–5 (leucrose), and 1–6 linked disaccharides (palatinose, melibiose, and gentiobiose) generate not only glycosidic cleavage ions but also cross-ring cleavage ions with differences in their relative intensities. The observation of a CID peak at m/z = 245 ($C_4H_8O_4$ loss) is characteristic of the 1–6 linked disaccharides: palatinose, gentiobiose, and melibiose, as indicated in Table 1.

Similar to the CID spectra, the VUVPD spectra provide structural information associated with linkage type and anomeric configuration of precursor ions. The $-C_4H_8O_4$ product ion at m/z = 245 is relatively abundant for the 1–6 linked disaccharides. The 1–4 and 1–5 linked disaccharides also exhibit this fragment ion at comparatively lower intensities.

3.3. Differentiation of anomers by MS^2 analysis of individual disaccharides

In the CID spectra, the α- and β-configuration of the glycosidic bonds in the 1–6 linked disaccharides can be distinguished by examining the relative intensity of the peak at m/z = 203. Two α anomers among the 1–6 linked disaccharides (melibiose and palatinose) present higher abundances of the ion at m/z = 203 compared to the fragment at m/z = 185 (Fig. 1). In contrast, the β anomer of the 1–6 linked disaccharide (gentiobiose) shows a very low intensity peak at m/z = 203. Irrespective of the linkage type, the other α anomers (leucrose, sucrose and trehalose) show consistently more abundant peaks at m/z = 203. The comparison of relative intensities of the peak at m/z = 203 to fragment at m/z = 185 provides a reliable means of anomeric differentiation.

VUVPD spectra show differences in relative intensities of the glycosidic cleavage ions at m/z = 202 and 203 that can be used to differentiate anomeric configuration among isobaric disaccharides. The product ion at m/z = 202 (C_1^{-1}/Y_1^{-1}) is a counterpart to the

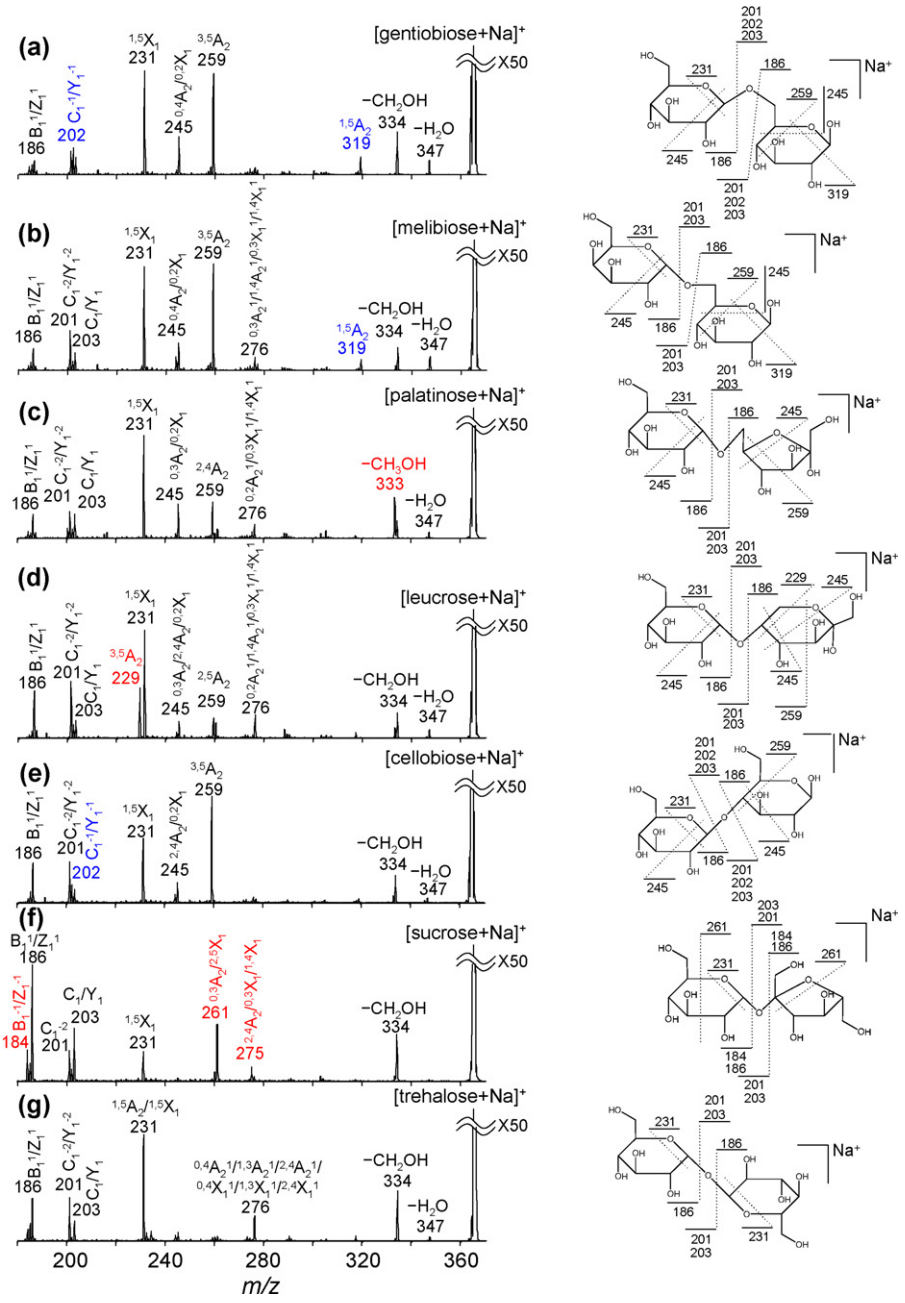

Fig. 2. VUVPD spectra of the $[M+Na]^+$ precursor ions. Spectra shown include: (a) gentiobiose (β1–6); (b) melibiose (α1–6); (c) palatinose (α1–6); (d) leucrose (α1–5); (e) cellobiose (β1–4); (f) sucrose (α1–2); and (g) trehalose (α1–1). Unique fragments for individual disaccharides are highlighted in red. Different combination of the peaks labeled in blue can be used to distinguish the isomers. Unique schematic representations of the VUVPD fragment ions (except ions at m/z = 275, 276, 333, 334, and 347 that are due to multiple possible cleavages) are shown on the molecular structures of individual disaccharides. All product ions are singly sodiated. (For interpretation of the references to color in this figure caption, the reader is referred to the web version of the article.)

Table 1
Mass spectral data of CID fragment ions for isobaric disaccharides.

m/z	Gentiobiose (β1–6)	Melibiose (α1–6)	Palatinose (α1–6)	Leucrose (α1–5)	Cellobiose (β1–4)	Sucrose (α1–2)	Trehalose (α1–1)
185	X	X		X	X	X	X
203	X	X	X	X	X	X	X
245	X	X	X				
275	X	X	X	X	X		
305	X	X	X	X	X		
347	X	X	X	X	X		

Table 2
Mass spectral data of photofragment ions for isobaric disaccharides.

m/z	Gentiobiose (β1–6)	Melibiose (α1–6)	Palatinose (α1–6)	Leucrose (α1–5)	Cellobiose (β1–4)	Sucrose (α1–2)	Trehalose (α1–1)
184						X	
186	X	X	X	X	X	X	X
201	X	X	X	X	X	X	X
202	X				X		
203	X	X	X	X	X	X	X
229				X			
231	X	X	X	X	X	X	X
245	X	X	X	X	X		
259	X	X	X	X	X		
261						X	
275,276[a]		X	X	X		X	X
319	X	X					
333			X				
334	X	X	X	X	X	X	X
347	X	X	X	X	X		X

[a] The ion at *m/z* = 276 is the H-transfer cross-ring cleavage ion of *m/z* = 275. In the VUVPD spectra, the ion at *m/z* = 275 is a unique fragment for sucrose.

fragment ion at *m/z* = 186 (B_1^1/Z_1^1) that is due to the homolytic cleavage of the glycosidic bond. For β anomers, the peak intensity at *m/z* = 202 is higher than that at *m/z* = 203. Both the CID and VUVPD spectra show that the linkage-bond cleavage on the side of the glycosidic oxygen is associated with α- and β-configuration of glycosidic bonds. Finally, the appearance of cross-ring cleavage ions at *m/z* = 276 (*m/z* = 275 for sucrose) indicates the α anomer (Table 2).

3.4. MS^3 analyses of individual disaccharides

Previous reports have indicated that higher-order tandem MS experiments provide additional structural information that can be used to identify precursor ions [12–16]. We previously showed that collisional activation of photofragment can help to identify them [24,39]. As another example of this strategy, the photofragment ions produced from palatinose and trehalose have been examined. The $-C_5H_{10}O_4$ fragment at *m/z* = 231 ($^{1,5}X_1$) obtained by VUVPD is a nonspecific, cross-ring cleavage ion for the seven isobaric disaccharides. CID spectra of the photofragment (*m/z* = 231) from the $[M+Na]^+$ palatinose and trehalose ions are shown in Fig. 3. The neutral loss of H_2O is a major fragment ion at *m/z* = 213 for the CID of the palatinose photofragment ion. Additionally, CID of the palatinose fragment ion generates several cross-ring cleavage ions at *m/z* = 113, 141, 155, and 171 corresponding to losses of $C_4H_6O_4$, $C_3H_6O_3$, $C_2H_4O_3$, and $C_2H_4O_2$ fragments, respectively (Fig. 3a). The ion at *m/z* = 155 is a structurally specific fragment ion for the $[M+Na]^+$ palatinose ions. Here, the loss of $C_2H_4O_3$ is possible if the disaccharide has OH and CH_3OH groups on the same ring carbon adjacent to the ring oxygen. In comparison to the MS^3 analysis of palatinose, CID of the trehalose photofragment ion results in simply the $-CH_2O_2$ ion at *m/z* = 185 (Fig. 3b). Probing the nonspecific photofragment with CID reveals different dissociation pathways that can be linked to the structures of the precursor ions.

In separate studies, the nonspecific product ion at *m/z* = 201 (Fig. 2) also shows different fragmentation patterns for the disaccharide isomers. Collisional activation of the trehalose photofragment ion at *m/z* = 201 shows products at *m/z* = 125, 141, 155, and 183. With the exception of the ion at *m/z* = 155, the same product ions are observed for the palatinose photofragment ion. The distinctive product ion (*m/z* = 155) in the MS^3 spectra can help to distinguish isomers when the MS^2 analysis is not sufficient.

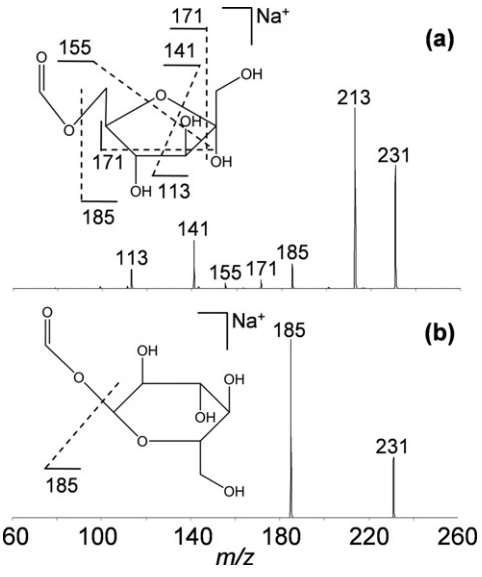

Fig. 3. CID spectra of the photofragment ion at *m/z* = 231 ($^{1,5}X_1$) produced by VUVPD of (a) palatinose (α1–6) and (b) trehalose (α1–1).

3.5. MS^2 analyses of disaccharide isomers separated by IMS

As described above, analysis of the individual CID spectra provides information for linkage type and anomeric configuration of isobaric disaccharides. However, for a mixture of the seven disaccharides studied here, isomer differentiation becomes a challenge using MS or MS^2 alone. The CID spectrum of the disaccharide mixture would show the combination of all the CID fragment peaks from each component (shown in Fig. 1) and most of these species appear at the same *m/z* values. Therefore, in order to identify sample components, an additional separation step is required prior to mass spectrometric analysis. That said, if the resolution of the additional separation step is not sufficient to base-line resolve each component, obtaining evidence for the presence of each isomer from the mixture could still be problematic due to the identical *m/z* values of the CID fragments.

Fig. 4a shows the drift time distribution for the $[M+Na]^+$ precursor ions from the seven component disaccharide mixture. The distribution contains features ranging from ~13.7 to ~15.4 ms and major features are observed at 13.98, 14.54, and 14.94 ms. The higher mobility feature at 13.98 ms is relatively well resolved from the other features. The middle and lower mobility features (14.54 and 14.94 ms, respectively) are partially resolved and include shoulders at 14.62 and 15.10 ms, suggesting the presence of several isomer ions under the broad features. Although isobaric

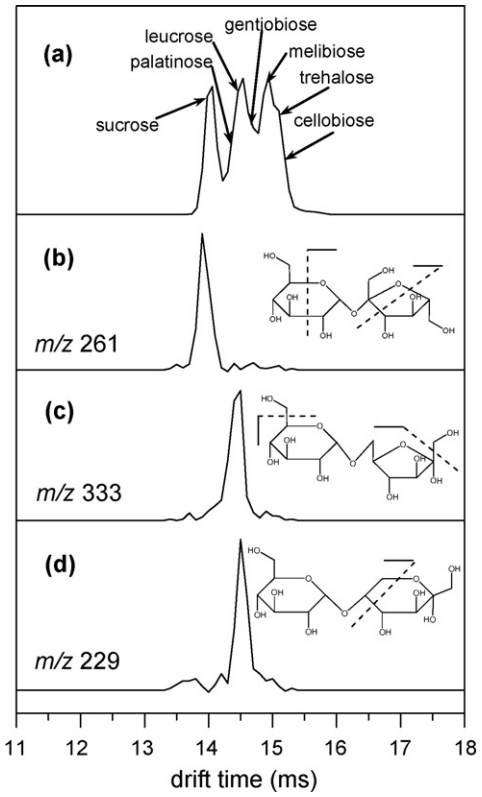

Fig. 4. (a) t_D distribution (XIDTD) of the $[M+Na]^+$ ions of seven disacharride components in a mixture. XFIDTDs obtained for the photofragments of the $[M+Na]^+$ ions of (b) sucrose, (c) palatinose, and (d) leucrose are also shown. Possible bond cleavages associated with the m/z value of the fragment used are shown on the molecular structure as an inset.

disaccharides are partially resolved in the mobility separation, IMS combined with MS alone or even MS^2 employing CID is insufficient to identify the individual isomers from the mixture.

For the seven disaccharides mixture, coupling mobility separations with VUVPD can alleviate the ambiguity in identifying mixture components. As described for the individual disaccharide analyses above, VUVPD generates unique fragments for most of the isobaric disaccharides. Here, we demonstrate that the distinctive product ions obtained by VUVPD can be utilized to reveal each mobility-selected isomer within the mixture. Additionally, a mobility distribution can be obtained by integrating the intensities of the unique fragment ion across a narrow m/z range at each drift selection time. As shown recently [40], the extracted fragment ion drift time distribution (XFIDTD) requires the presence of the precursor ions. Thus, the distribution can be representative of the ion mobility distribution of the precursor ion. Because the isobaric mixture is comprised of ions of similar mobilities (consequently they are partially resolved in Fig. 4a) and all mixture components have identical mass, it is difficult to assign their relative mobilities from an IMS–MS analysis alone. The XFIDTD is sufficient to determine the exact mobility of a specific component within a mixture.

Three unique fragments at m/z = 184, 261, and 275 can be used as a molecular fingerprint to identify sucrose. The VUVPD spectra of mobility-selected ions across the higher mobility feature (13.98–14.14 ms) show fragmentation patterns identical to the individual VUVPD spectrum of sucrose (Fig. 2f) including the three distinctive product ions. The photofragment at m/z = 261 is the most abundant among the unique fragments and thus it can be used to generate a t_D distribution for sucrose precursor ions within the mixture (Fig. 4b). The XFIDTD shows one feature centered at ~13.98 ms. These results confirm that the mixture contains sucrose existing as the highest mobility ion among the seven disaccharides.

As the drift selection time increases above 14.22 ms, the fragmentation pattern upon photoexcitation changes. At a drift selection time of 14.38 ms, the three unique ions for sucrose are not observed in the VUVPD spectrum and the fragment ion at m/z = 333 becomes pronounced indicating the presence of palatinose. Additionally, a small peak at m/z = 229 corresponding to the structurally specific fragment of the $[M+Na]^+$ leucrose ions is observed. As the drift selection time increases by 80 μs, the characteristic product ion for leucrose becomes one of the main fragments and the unique ion for palatinose becomes smaller. The XFIDTDs for the palatinose and leucrose are obtained by extraction of the data for the unique photofragments at m/z = 333 and 229, respectively (Fig. 4c and d). The XFIDTDs of palatinose and leucrose show single features centered at ~14.46 and ~14.54 ms, respectively. These suggest that palatinose is the next highest mobility component in the disaccharide mixture followed by leucrose.

Next, distinctive fragments for the ions at m/z = 202 and 319 are observed, as the drift selection time increases by 160 μs. Based on individual VUVPD spectra (Fig. 2), the peak at m/z = 202 is more noticeable compared with the peak at m/z = 203 for the β anomers which narrows identification down to cellobiose and gentiobiose. In addition to the ion at m/z = 202, the peak at m/z = 319 observed only in the individual VUVPD analysis of melibiose and gentiobiose indicates that the mobility selection from the mixture at 14.62 ms corresponds to gentiobiose. At 14.86 ms, the ion at m/z = 202 vanishes, but the ion at m/z = 319 remains with a similar intensity. These results suggest that the mobility of the $[M+Na]^+$ gentiobiose ions is slightly higher than that of the $[M+Na]^+$ melibiose ions.

From the disaccharide mixture, the VUVPD spectrum obtained at a drift selection time of 15.10 ms shows a very similar fragmentation pattern to that of the $[M+Na]^+$ melibiose ions (Fig. 2). At a drift selection time of 15.18 ms, the peak at m/z = 202 appears again, but now without the ion at m/z = 319, thus indicating the presence of cellobiose in the mixture. A close inspection of the mobility-dependent VUVPD spectra reveals that the intensity of the peak at m/z = 259 obtained from a selection at 15.10 ms is lower than those at 14.86 and 15.18 ms. As mentioned above, the ion at m/z = 259 is not observed in the VUVPD spectrum of the $[M+Na]^+$ trehalose ions, while the product ion is the most dominant peak for the $[M+Na]^+$ melibiose and cellobiose ions. Therefore, the intensity decrease of the peak at m/z = 259 at 15.10 ms may result from the absence of this trehalose ion. To verify the presence of trehalose at 15.10 ms, MS^3 analysis has been employed. The CID spectrum of the photofragment at m/z = 201 obtained by selecting mobility ions at 15.10 ms shows a distinctive ion at m/z = 155 that is not shown in the MS^3 spectra of the melibiose and cellobiose product ions.

In summary, the observation of distinctive peaks for each disaccharide isomer along the ion mobility distribution is helpful to identify individual components from the mixture. As shown in Fig. 4a, VUVPD of the mobility selected ions at 13.98, 14.38, 14.46, 14.62, 14.86, and 15.18 ms produces specific fragment ions for the $[M+Na]^+$ sucrose, palatinose, leucrose, gentiobiose, melibiose, and cellobiose ions, respectively. Because no unique fragment is observed for the $[M+Na]^+$ trehalose ions, it is somewhat ambiguous to demonstrate its presence in the mixture. However, as described above, the fragmentation patterns resulting in different relative intensities and the MS^3 analysis can be used as complementary information to differentiate such a component from the mixture.

With the current instrumental apparatus it is not possible to quantify the mixture components because of the overlap in the mobility dimension and the fact that unique fragments may be formed in very different abundance levels as compared to the relative abundances of the precursor ions. That said, high-resolution IMS techniques (which show baseline-resolved peaks for the

precursor ions) would allow quantitative analyses. Thus, the improved mobility separation combined with VUVPD has potential for both quantitative and qualitative analyses of complex mixtures. It is noteworthy that the proof-of-principle demonstration here can be extended by the use of statistical analysis techniques (e.g., principal component analysis) to verify the presence of particular isomers within more complex mixtures. This may have implications for comparative profiling experiments such as those found in glycomics studies.

4. Conclusion

Both CID and VUVPD have shown linkage- and anomeric configuration-dependent dissociation patterns for the isobaric disaccharides. More complicated fragmentation involving reducing and nonreducing cross-ring cleavages is observed from the VUV PD experiments. Additionally, VUVPD generates distinctive photofragments for most of the disaccharides, which are valuable in differentiating individual components within a mixture. Incorporation of the gas-phase mobility separation helps to distinguish isomers having identical m/z values prior to MS^n analysis. Coupling mobility separations with VUVPD experiments allows identification of disaccharide isomers within the mixture as well as a means to pinpoint the $[M+Na]^+$ precursor ion mobilities. The combined techniques show promise for applications in the study of complex mixtures containing oligosaccharides or glycans.

Acknowledgment

The authors acknowledge support for the development of new instrumentation by a grant from the National Institutes of Health (1RC1GM090797-01).

References

[1] A. Krogh, J. Lindhard, The relative value of fat and carbohydrate as source of muscular energy, Biochem. J. 14 (1920) 290–363.
[2] K.C. Gross, C.E. Sams, Changes in cell wall neutral sugar composition during fruit ripening: a species survey, Phytochemistry 23 (1984) 2457–2461.
[3] D.W. Abbott, E. Ficko-Blean, A.L. van Bueren, A. Rogowski, A. Cartmell, P.M. Coutinho, B. Henrissat, H.J. Gilbert, A.B. Boraston, Analysis of the structural and functional diversity of plant cell wall specific family 6 carbohydrate binding modules, Biochemistry 48 (2009) 10395–10404.
[4] J.M. De la Fuente, S. Penades, Understanding carbohydrate–carbohydrate interactions by means of glyconanotechnology, Glycoconjugate J. 21 (2004) 149–163.
[5] S. Hakomori, Structure, organization, and function of glycosphingolipids in membrane, Curr. Opin. Hematol. Rev. 10 (2003) 16–24.
[6] M. Soric, A. Longo, T. Garofalo, V. Mattei, R. Misasi, A. Pavan, Role of GM3-enriched microdomains in signal transduction regulation in T lymphocytes, Glycoconjugate J. 20 (2004) 63–70.
[7] J.W. Dennis, M. Granovsky, C.E. Warren, Protein glycosylation in development and disease, Bioessays 21 (1999) 412–421.
[8] R. Kornfeld, S. Kornfeld, Assembly of asparagine-linked oligosaccharides, Annu. Rev. Biochem. 54 (1985) 631–664.
[9] Z. Xiao, B.R. Tappen, M. Ly, W. Zhao, L.P. Canova, H. Guan, R.J. Linhardt, Heparin mapping using heparin lyases and the generation of a novel low molecular weight heparin, J. Med. Chem. 54 (2011) 603–610.
[10] I.E. Alcamo, Anatomy and Physiology The Easy Way, vol. 386, 2nd ed., Barron's Educational Series, Inc., Hauppauge, NY, 2004.
[11] G.E. Hofmeister, Z. Zhou, J.L. Leary, Linkage position determination in lithium-cationized disaccharides: tandem mass spectrometry and semiempirical calculations, J. Am. Chem. Soc. 113 (1991) 5964–5970.
[12] M.R. Asam, G.L. Glish, Tandem mass spectrometry of alkali cationized polysaccharides in a quadrupole ion trap, J. Am. Soc. Mass Spectrom. 8 (1997) 987–995.
[13] J.M. Prien, D.J. Ashline, A.J. Lapadula, H. Zhang, V.N. Reinhold, The high mannose glycans from bovine ribonuclease B isomer characterization by ion trap MS, J. Am. Soc. Mass Spectrom. 20 (2009) 539–556.
[14] J. Jiao, H. Zhang, V.N. Reinhold, High performance IT-MS^n sequencing of glycans spatial resolution of ovalbumin isomers, Int. J. Mass Spectrom. 303 (2011) 109–117.
[15] J.M. Prien, L.C. Huysentruyt, D.J. Ashline, A.J. Lapadula, T.N. Seyfried, V.N. Reinhold, Differentiating N-linked glycan structural isomers in metastatic and nonmetastatic tumor cells using sequential mass spectrometry, Glycobiology 18 (2008) 353–366.
[16] Y. Wang, S.-I. Wu, W.S. Hancock, Approaches to the study of N-linked glycoproteins in human plasma using lectin affinity chromatography and nano-HPLC coupled to electrospray linear ion trap-Fourier transform mass spectrometry, Glycobiology 16 (2006) 514–523.
[17] C.J. Taylor, R.M. Burke, B. Wu, S. Panja, S.B. Nielsen, C.E.H. Dessent, Structural characterization of negatively charged glycosaminoglycans using high-energy (50–150 keV) collisional activation, Int. J. Mass Spectrom. 285 (2009) 70–77.
[18] H.J. An, S. Miyamoto, K.S. Lancaster, C. Kirmiz, B. Li, K.S. Lam, G.S. Leiserowitz, C.B. Lebrilla, Profiling of glycans in serum for the discovery of potential biomarkers for ovarian cancer, J. Proteome Res. 5 (2006) 1626–1635.
[19] J.J. Wolff, F.E. Leach, T.N. Laremore, D.A. Kaplan, M.L. Easterling, R.J. Linhardt, I.J. Amster, Negative electron transfer dissociation of glycosaminoglycans, Anal. Chem. 82 (2010) 3460–3466.
[20] J.T. Adamson, K. Hakansson, Electron capture dissociation of oligosaccharides ionized with alkali, alkaline earth, and transition metals, Anal. Chem. 79 (2007) 2901–2910.
[21] S.E. Stefan, J. Eyler, Differentiation of glucose-containing disaccharides by infrared multiple photon dissociation with a tunable CO_2 laser and Fourier transform ion cyclotron resonance mass spectrometry, Int. J. Mass Spectrom. 297 (2010) 96–101.
[22] Y. Liu, D.E. Clemmer, Characterizing oligosaccharides using injected-ion mobility/mass spectrometry, Anal. Chem. 69 (1997) 2504–2509.
[23] J.J. Wilson, J.S. Brodbelt, Ultraviolet photodissociation at 355 nm of fluorescently labeled oligosaccharides, Anal. Chem. 80 (2008) 5186–5196.
[24] A. Devakumar, Y. Mechref, P. Kang, M.V. Novotny, J.P. Reilly, Identification of isomeric n-glycan structures by mass spectrometry with 157 nm laser-induced photofragmentation, J. Am. Soc. Mass Spectrom. 19 (2008) 1027–1040.
[25] A. Devakumar, M.S. Thompson, J.P. Reilly, Fragmentation of oligosaccharide ions with 157 nm vacuum ultraviolet light, Rapid Commun. Mass Spectrom. 19 (2005) 2313–2320.
[26] K. Hakansson, H.J. Cooper, M.R. Emmett, C.E. Costello, A.G. Marshall, C.L. Nilsson, Electron capture dissociation and infrared multiphoton dissociation MS/MS of an N-glycosylated tryptic peptide to yield complementary sequence information, Anal. Chem. 73 (2001) 4530–4536.
[27] P.J. Oefner, C. Chiesa, Capillary electrophoresis of carbohydrates, Glycobiology 4 (1994) 397–412.
[28] A. Paulus, A. Klockow, Detection of carbohydrates in capillary electrophoresis, J. Chromatogr. A 720 (1996) 353–376.
[29] J.P. Williamsa, M. Grabenauerb, R.J. Hollandc, C.J. Carpenterb, M.R. Wormaldd, K. Gilese, D.J. Harveyd, R.H. Batemane, J.H. Scrivensc, M.T. Bowers, Characterization of simple isomeric oligosaccharides and the rapid separation of glycan mixtures by ion mobility mass spectrometry, Int. J. Mass Spectrom. 298 (2010) 119–127.
[30] B.H. Clowers, P. Dwivedi, W.E. Steiner, H.H. Hill, B. Bendiak, Separation of sodiated isobaric disaccharides and trisaccharides using electrospray ionization–atmospheric pressure ion mobility–time of flight mass spectrometry, J. Am. Soc. Mass Spectrom. 16 (2005) 660–669.
[31] W. Gabryelski, K. Froese, Rapid and sensitive differentiation of anomer, linkage, and position isomers of disaccharides using high-field asymmetric waveform ion mobility spectrometry (FAIMS), J. Am. Soc. Mass Spectrom. 14 (2003) 265–277.
[32] D.E. Clemmer, M.F. Jarrold, Ion mobility measurements and their applications to clusters and biomolecules, J. Mass Spectrom. 32 (1997) 577–592.
[33] G. von Helden, T. Wyttenbach, M.T. Bowers, Conformation of macromolecules in the gas phase: use of matrix-assisted laser desorption methods in ion chromatography, Science 267 (1995) 1483–1485.
[34] K.J. Gillig, B. Ruotolo, E.G. Stone, D.H. Russell, K. Fuhrer, M. Gonin, A.J. Schultz, Coupling high pressure MALDI with ion mobility/orthogonal time-of-flight mass spectrometry, Anal. Chem. 72 (2000) 3965–3971.
[35] T. Wyttenbach, G. von Helden, J.J. Batka, D. Carlat, M.T. Bowers, Effect of the long-range potential on ion mobility measurements, J. Am. Soc. Mass Spectrom. 8 (1997) 275–282.
[36] A.A. Shvartsburg, M.F. Jarrold, An exact hard-spheres scattering model for the mobilities of polyatomic ions, Chem. Phys. Lett. 261 (1996) 86–91.
[37] E.A. Mason, E.W. McDaniel, Transport Properties of Ions in Gases, Wiley, New York, 1988.
[38] H.E. Revercomb, E.A. Mason, Theory of plasma chromatography/gaseous electrophoresis—a review, Anal. Chem. 47 (1975) 970–983.
[39] S.M. Zucker, S. Lee, N. Webber, S.J. Valentine, J.P. Reilly, D.E. Clemmer, An ion mobility/ion trap/photodissociation instrument for characterization of ion structure, J. Am. Soc. Mass Spectrom. 22 (2011) 1477–1485.
[40] S. Lee, Z. Li, S.J. Valentine, S.M. Zucker, N. Webber, J.P. Reilly, D.E. Clemmer, Extracted fragment ion mobility distributions: a new method for complex mixture analysis, Int. J. Mass Spectrom 309 (2012) 161–167.
[41] S.A. Shaffer, D.C. Prior, G.A. Anderson, H.R. Udseth, R.D. Smith, An ion funnel interface for improved ion focusing and sensitivity using electrospray ionization mass spectrometry, Anal. Chem. 70 (1998) 4111–4119.
[42] B. Domon, C.E. Costello, A systematic nomenclature for carbohydrate fragmentations in FAB-MS/MS spectra of glycoconjugates, Glycoconjugate J. 5 (1988) 397–409.